# CHARACTERISATION OF ADAPTIVE FLUIDIC SILICONE-MEMBRANE LENSES

**F. Schneider[1,2],J. Draheim[2], J. Brunne[2], P. Waibel[2] and U. Wallrabe[2]**

[1] *Material Science and Manufacturing, CSIR, PO Box 395, Pretoria, 0001, South Africa.*
*Email: florian.schneider@imtek.uni-freiburg.de*
[2] *Department of Microsystems Engineering – IMTEK, University of Freiburg, Georges-Koehler-Allee 102, Freiburg, 79110, Germany.*

**Abstract:** We compare the performance and optical quality of two types of adaptive fluidic silicone-membrane lenses. The membranes feature either a homogeneous thickness, or they are shaped resulting in an inhomogeneous cross-section. The lens systems incorporate a piezoelectric actuator which is operated in a regime of ±40 V. The shaped membrane lenses show lower wave front errors than the planar ones, down to 24 nm. The pumping actuator indicates a maximum pump volume of 1159 nl at an inner piezo radius of 2.75 mm for the smallest supporting ring configuration. The full system with a planar membrane achieves a larger refractive power ranging from +19 to -14 dpt. It also shows a shorter full scale response time ($t_{planar}$ = 23.9 ms) compared to the shaped membrane ($t_{shaped}$ = 35.4 ms).

**Key words:** adaptive optics, piezoelectric actuator, silicone

## 1. INTRODUCTION

The development of adaptive lenses increased drastically over the last few years. In contrast to conventional systems with mechanical moving parts, adaptive lenses show no mechanical wear, however they are costly. In the meantime, three lenses based on different working principles are commercially available. The first one is the electrowetting lens of Varioptics. The lens with a clear aperture of 2.5 mm is developed for the main application in consumer electronics (mobile phones, PDAs, laptops) [1]. The second lens of Optotune has an aperture of 6 mm in diameter and is mostly suitable for digital cameras and microscopes. The adaptive lens is based on an electroactive polymer, which deforms an elastic lens [2]. The third product is available at Holochip and consists of a fluid-based singlet lens, where the interface is set by an elastic silicone membrane. The focal length of the lens with an aperture of 10 mm is tunable by the mechanical moving of the clamping ring [3].
As an alternative to the commercially available lenses we have recently presented an adaptive silicone membrane lens with an integrated piezoelectric pump for actuation. The lens is suitable for the use in optical systems with a clear aperture of 2.5 mm [4, 5]. In this paper we focus on the characterisation of the single components (lens and pump actuator) and the full system for lenses with planar and shaped membranes.

## 2. ASSEMBLY AND FABRICATION

The system consists of two components: a lens and a pump actuator, which are connected via a glass substrate (see figure 1). The lens chamber is filled with water or immersion oil, and consists of a silicone membrane with a homogeneous or an inhomogeneous thickness, and of a supporting ring (see figure 2).

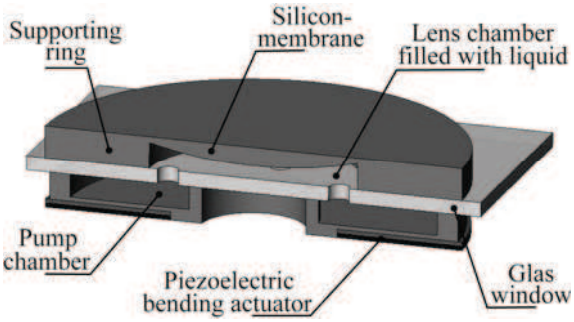


Figure 1: Adaptive liquid lens with an integrated piezoelectric actuator.

The pump chamber, which is also filled with liquid, is made up of a piezoelectric bending actuator embedded in silicone. The exchange of liquid between the pump and lens chamber is enabled by orifices in the glass substrate. If a voltage is applied to the piezo-bending actuator, its interior bulges upwards so that the lens fluid is displaced from the pump chamber into the lens chamber. This causes a growing bulge of the lens membrane and thus a reduction in the focal length of the lens.

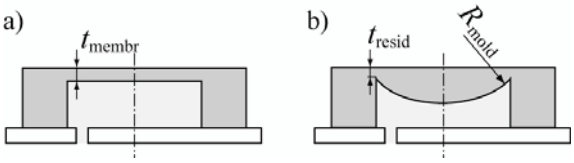


Figure 2: Membrane variations, lens chamber with a) planar and b) shaped membrane.

The lens and the pump chamber are fabricated with a surface roughness of $R_a < 40$ nm in polydimethyl-siloxane (PDMS). The two chambers are cast in a hot embossing machine. In the fabrication process, a brass

substrate produced by ultra-precision milling (UPM) is used as mold. Exemplarily the fabrication process of the lens chamber is shown in figure 3. In case of a homogenously thick membrane, the membrane thickness $t_{membr}$ is controlled by a spacer ring located between the brass mold and the polycarbonate foil. Additionally, for the inhomogeneous membrane we place concave shaped lenses in the mold. Generally, the volume shrinkage of the silicone is counteracted by the stamp force during the hardening process in the hot embossing machine. Since this force, however, is constant for all membrane thicknesses, the volume shrinkage for several membrane thicknesses increases with the cube of the membrane thickness.

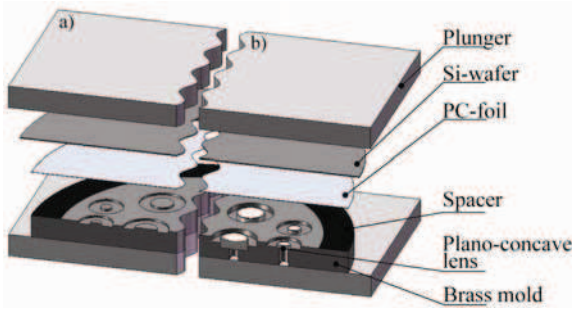


Figure 3: Fabrication process in a hot embossing machine for a lens chamber with a) a planar and b) a shaped membrane.

## 3. CHARACTERIZATION

This chapter is devoted to the characterisation of the single components and the full system. The simulation and measurement of the optical lens quality is realized by a FE- and ray tracing simulation and a Mach-Zehnder interferometrical setup. The pump volume of the piezoelectric bending actuator is optimized by FE-simulation and a laser-profilometer. For the full system we are analyzing the refraction power as a function of the piezo voltage and the dynamical behavior as well.

### *3.1 Optical lens quality*

The optical lens quality of the opto-mechanical component is analyzed by a mechanical FE-simulation and ray tracing. In order to judge the lens quality, we examined the wave front error ($WFE_{RMS}$) of the different membrane shapes in a horizontal lens orientation. For the PDMS we set an elastic modulus of 1.54 MPa [6], a Poisson ratio of 0.49 and a refractive index of 1.4282 [6]. As lens liquid we use water with a refractive index of 1.33.

Figures 4 shows the wave front error in RMS as a function of the focal length for lenses with homogeneous membranes in horizontal orientation. Generally, the wave front error is decreasing for increasing focal length and decreasing membrane thickness. The influence of the membrane thickness is traced back to the reduction of the membrane stiffness which shifts the inflection point of the membrane in the direction of the membrane fixation, which reduces the spherical aberration. In the horizontal orientation the hydrostatic pressure of the lens fluid increases the membranes radius of curvature and decreases the spherical aberration, which results in a rising lens performance.

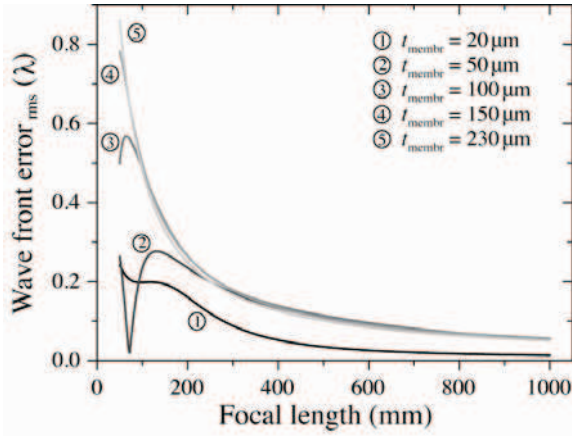


Figure 4: Simulated aberration of the planar membrane lens as a function of the focal length. $d_{lens}$ = 5 mm, $d_{ap}$ = 2.5 mm

For the lenses with inhomogeneous membranes the influence of the residual membrane thickness $t_{resid}$ (see figure 2b) at 10 mm radius of curvature $R_{mold}$ is investigated (see figure 5). The curves show the smallest aberration in the non-deflected initial state at a focal length of 125 mm. For deflected situations (increasing or decreasing focal length) the wave front errors increase drastically with a decreasing residual membrane thickness due to a more inhomogeneous membrane deformation.

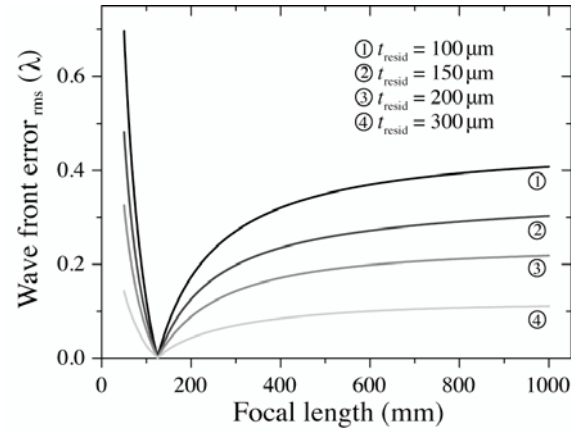


Figure 5: Simulated aberration of the shaped membrane as a function of the focal length. $d_{lens}$ = 5 mm, $d_{ap}$ = 2.5 mm, $R_{mold}$ = 10 mm

For experimental characterization of the optical lens quality we measure the wave front error ($WFR_{RMS}$) at a wave length of 633 nm by using a Mach-Zehnder interferometer. The detailed configuration of the interferometer is given in [7]. Figure 6 shows the

measurement results of the lenses with homogenous membranes as a function of the focal length for different membrane thicknesses at an aperture of 2.125 mm. The diagram shows a minimal wave front error in RMS of 0.047 λ for a membrane thickness of 50 µm at a focal length of 800 mm. In general, the curve shapes of the measurements and the simulations without volume shrinkage (see figure 4) are in a good correlation.

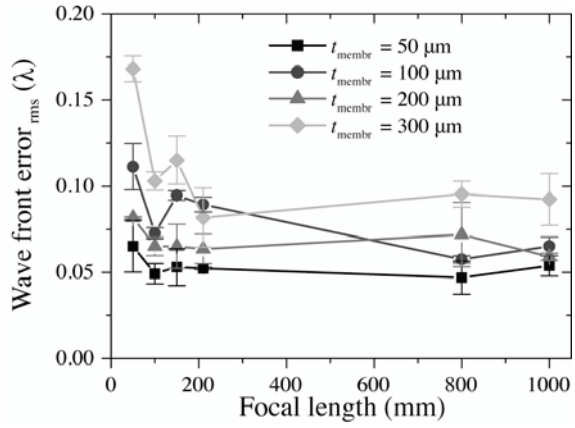


Figure 6: Measured aberration of the planar membrane lens as a function of the focal length. $d_{lens}$ = 5 mm, $d_{ap}$ = 2.125 mm

Figure 7 shows the measurement result of the inhomogeneous membrane lens for diverse residual membrane thicknesses at a mold radius of curvature of 9.3 mm. All curves illustrate a minimal aberration at a focal length of 66 mm. The wave front error is increasing for decreasing membrane thickness and deflection of the membrane. In comparison to the homogeneous membrane the minimum wave front error could be reduced to 0.037 λ. The trend of the measurement curves are in good correlation to the simulated behavior without volume shrinkage (see figure 5).

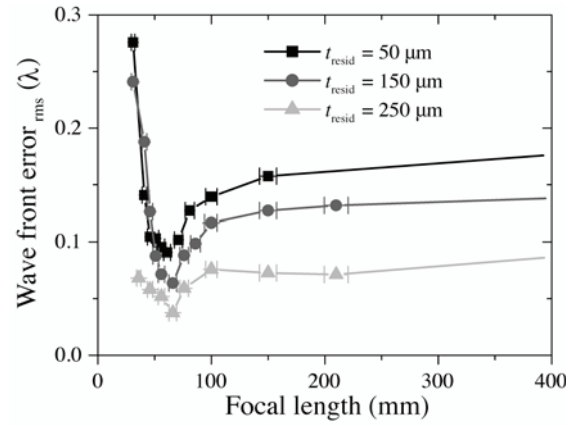


Figure 7: Measured aberration of the shaped membrane as a function of the focal length. $d_{lens}$ = 6 mm, $d_{ap}$ = 2.125 mm, $R_{mold}$ = 9.3 mm

The difference between the simulation and the measured focal length in the initial state can be traced back to the volume shrinkage of the silicone during the fabrication process which let the focal length decrease.

*3.2 Pump actuator*

This paragraph is devoted to the optimization of the piezoelectric pump. For this purpose we concentrate on the maximization of the pump volume by using FE-simulation. Therefore, the influence of the inner piezo radius $r_{piezo}$ and the inner and outer supporting ring width $\Delta r$ are analyzed (see figure 8).

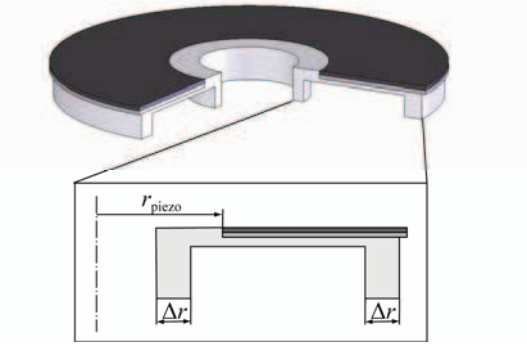


Figure 8: Parameter model of the piezoelectric pumping actuator.

Figure 9 shows the pump volume as a function of the inner piezo radius for diverse supporting ring width $\Delta r$ at an applied voltage of -40 V. A maximum volume of 1405 nl is displaced at a inner piezo radius of 2810 µm for the thinnest supporting ring configuration. A reduction in the effectiveness of the pump with small inner piezo radii can be attributed to an elevated mechanical stiffness in the inner supporting ring. On the other hand, with larger radii the pump volume decreases due to the declining length of the bending actuator. The pumping volume is decreasing for increasing supporting ring width, due to the increasing stiffness of the actuator fixation.

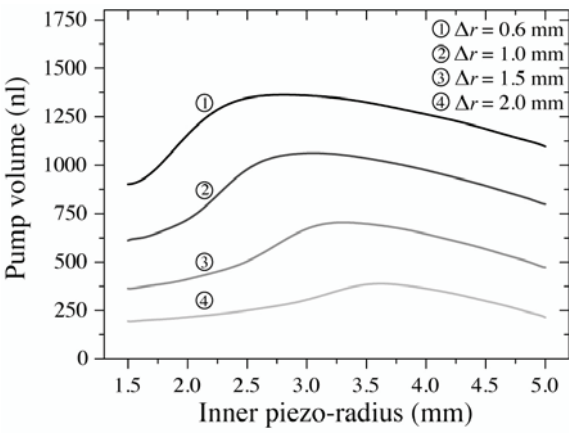


Figure 9: Simulation of the displaced pump volume as a function of the inner piezo radius $r_{piezo}$ for diverse supporting ring width at -40 V.

The measurement of the pump volume is realized by a laser-profilometer. After a surface scan of the piezoelectric actuator at a voltage of -40 V the pump volume is calculated. Exemplarily, figure 10 shows the measurement result for a two different supporting ring widths of 600 and 1000 µm. On the one hand, the maximum pump volume for the actuator with the thinner supporting ring is 1159 nl at an inner piezo radius of 2.75 mm. On the other hand, the displaced volume for the configuration with the thicker supporting ring is decreasing down to 892 nl at a inner piezo radius of 3.25 mm. The curve shapes of the measurement and the simulation are in a good correlation. The difference in the pump volume can be traced back to the volume shrinkage of the silicone which increases the supporting ring stiffness. Otherwise, the process related internal stress in the piezoelectric bending actuator reduces the displaced volume as well.

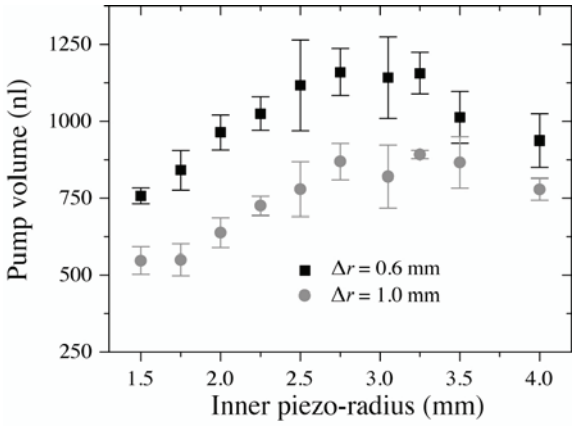


Figure 10: Measurement result of the displaced pump volume as a function of the inner piezo radius $r_{piezo}$ for different supporting ring width $\Delta r$ at -40 V.

*3.3 System performance*

For the full system we want to know the refraction power as a function of the piezo voltage. In the simulation the interaction of the lens chamber to the pump performance has been considered. In a first simulation step, the lens back pressure as a function of the lens volume, respectively the focal length has been simulated. In the second step we calculated the pump volume of the actuator as a function of the piezo voltage inclusive lens back pressure in an iterative simulation. Finally, the pump volume of the actuator and the lens volume are set equal to link the focal length to the piezo voltage. Exemplarily, figure 11 shows the system performance of lenses with homogeneous membranes between a thickness of 20 and 230 µm. The maximum refraction power range is not achieved for the thinnest membrane as one would actually expect but for a medium membrane thickness of 150 µm. This is related to two opposing effects. On the one hand, the actuator simulation inclusive lens backpressure shows a decreasing pump volume for an increasing membrane thickness.

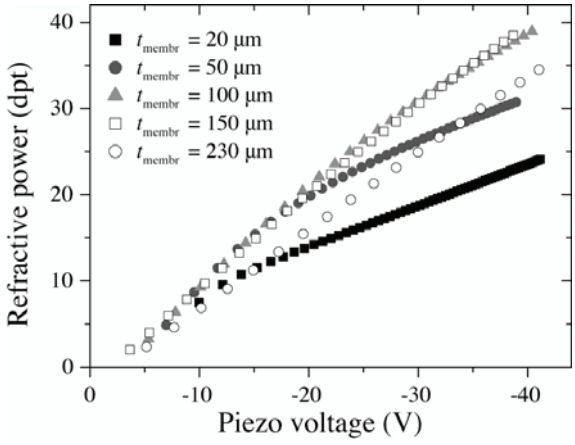


Figure 11: Simulated refractive power as a function of the piezo voltage for different homogeneous membrane thicknesses $t_{membr}$.

On the other hand, with decreasing membrane thickness the radius of curvature increase, as can be seen in figure 12, due to the shift of the membrane inflection point.

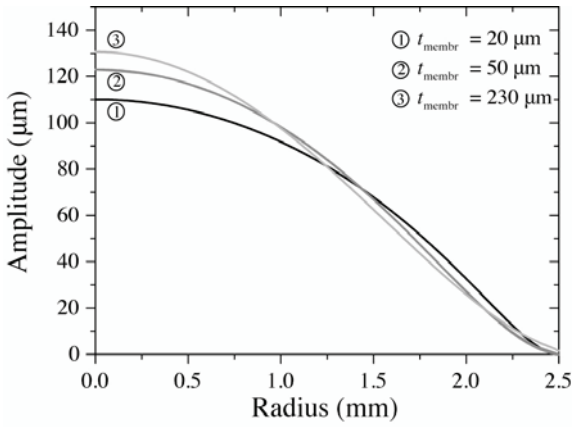


Figure 12: Simulated membrane shapes for a lens volume of 1 µl at divorce homogeneous membrane thicknesses.

The measurement of the system behaviour is realized by the laser-profilometer in the dynamic mode. For the lens with a homogeneous membrane the membrane surface profile is measured and the refraction power of the lens is calculated subsequently. Additionally, for the membranes with an inhomogeneous form the shape of the membrane backside is calculated via FE-simulation. Figure 13 displays the measured refractive power as a function of the piezo voltage at a frequency of 1 Hz. The system with the planar membrane show a refractive power range of +19 to -14 dpt, and the shape one a range of +9…+1 dpt. The reduced refractive power range of the system with an inhomogeneous lens membrane arises from the increasing membrane stiffness, respectively the increasing back pressure to the pump actuator. The big difference between the simulation result and measurements can be traced back to the volume shrinkage of the silicone which in not considered in the simulation. The hysteresis curve

shape at the measurements is typically for piezoelectric actuators.

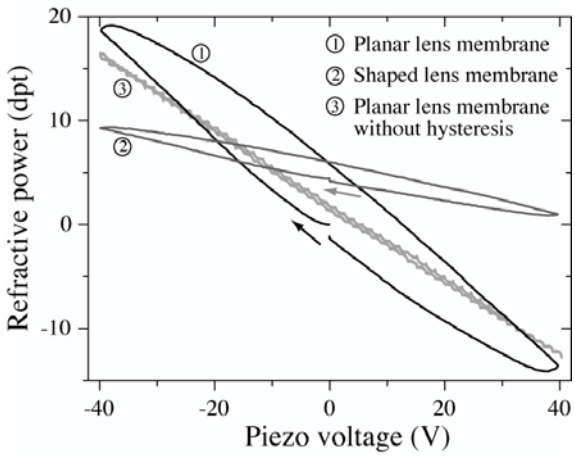


Figure 13: Measured refractive power as a function of the piezo voltage for a system with a planar ($t_{membr}$ = 60 µm) and a shaped ($t_{resid}$ = 75 µm, $R_{mold}$ = 9.3 mm) lens membrane.

In order to reduce the hysteresis we operate the piezoelectric actuator dynamically. First, a piezo voltage $U_{piezo}$ is applied to the actuator for a time of 15 ms. Afterwards, the whole hysteresis curve is run through in 60 µs. Thereby, the lens membrane can not follow the actuator movement, due to the high damping of the lens membrane. Exemplarily, figure 13 also shows the drastic hysteresis reduction for the lens with a homogeneous membrane thickness. The hysteresis can be suppressed down to a maximum residual of 0.5 dpt.

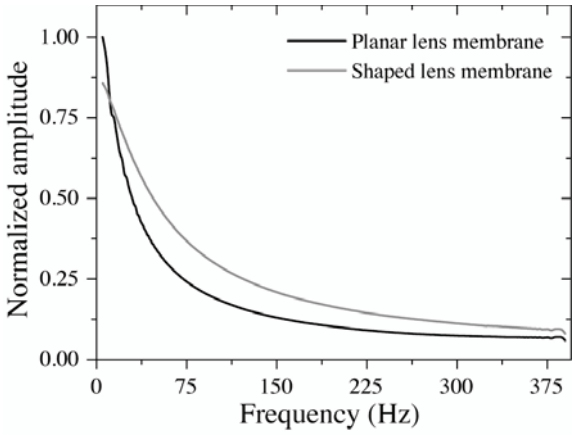


Figure 14: Measured frequency response for a system with a planar ($t_{membr}$ = 60 µm) and a shaped ($t_{resid}$ = 75 µm, $R_{mold}$ = 9.3 mm) lens membrane.

For the dynamical characterization we measure the frequency response (see figure 14) and the full scale response time. The system with a shaped lens membrane shows a more direct response characteristic than a system with a planar membrane, due to the lower membrane amplitude. The full scale response time is measured at a voltage step from +40 to -40 V and reverse. The system with a planar membrane indicates an isotropic response time of 23.9 ms and the lens with a shaped membrane a time of 35.4 ms. This arises from the higher lens back pressure of the inhomogeneous membrane, which let the response time increase.

## 4. CONCLUSIONS

The use of adaptive lens systems with homogeneous, respectively, inhomogeneous membranes is application specific. On the one hand, systems with planar membranes are reasonable for a large focal length range, a constant optical lens quality and a short response time. On the other hand, the application of lenses with shaped membranes is reasonable for a higher optical lens quality at a smaller focal length range around a working point.

## 5. REFERENCES

[1] B. Berge and J. Peseux: "Variable focal lens controlled by an external voltage: an application of electrowetting," *Eur. Phys. J. E,* Vol. 3, pp. 159-163 2000.

[2] Optotune: "Electrical focus tunable lens EL-6-22," *Datasheet*, 2008.

[3] H. Ren, D. Fox, P. A. Anderson, B. Wu and S.-T. Wu: "Tunable-focus liquid lens controlled using a servo motor," *Opt. Express*, Vol. 14, pp. 8031-8036, 2006.

[4] F. Schneider, C. Müller and U. Wallrabe: "A low cost adaptive silicone membrane lens," *J. Opt. A: Pure Appl. Opt.,* Vol. 10, 044002, 2008.

[5] F. Schneider, J. Draheim, C. Müller and U. Wallrabe: "Optimization of an adaptive PDMS-membrane lens with an integrated actuator," *Sens. Actuators A: Phys.*, doi:10.1016/j.sna.2008.07.006, 2008.

[6] F. Schneider, J. Draheim, R. Kamberger and U. Wallrabe: "Process and material properties of polydimethysiloxane (PDMS) for Optical MEMS," *Sens. Actuators A: Phys.*, Vol. 151, pp. 95-99, 2009.

[7] S. Reichelt and H. Zappe: "Combined Twyman–Green and Mach–Zehnder interferometer for microlens testing," *Appl. Opt.*, Vol. 44, pp. 5786-5792 (2005).